Chemical Engineering Journal 151 (2009) 302–307

Contents lists available at ScienceDirect

Chemical Engineering Journal

journal homepage: www.elsevier.com/locate/cej

Mass transfer and thermodynamic aspects of sodium desorption from eucalyptus kraft pulp by acidification using carbon dioxide

Denny Vitasari*, Kien L. Nguyen, Vinh Dang

Australian Pulp and Paper Institute, Department of Chemical Engineering, Monash University, Clayton VIC 3800, Australia

ARTICLE INFO

Article history:
Received 10 June 2008
Received in revised form 28 February 2009
Accepted 5 March 2009

Keywords:
Pulp acidification
Desorption
Carbon dioxide
Eucalyptus
Kraft pulp

ABSTRACT

The thermodynamics and mass transfer aspects associated with the use of CO_2 for the acidification, particularly for the removal of Na^+ from pulp fibres, were studied. The acidifications with CO_2 and with H_2SO_4 were carried out in a stirred tank reactor under different temperatures, agitation speeds, concentrations of CO_2 and H_2SO_4 and treatment times. The CO_2 acidification of pulp was found to be very fast at $Re > 10^4$ and N_p of 4, and reached equilibrium within 5 min. The volumetric mass transfer coefficient, k_La, of the CO_2 acidification was found to be in the range of 0.0005–0.0083 s^{-1}. Thermodynamically, the CO_2 acidification was achievable only at pH > 4. The extent of the resultant Na^+ exchange increased with the acidification time, agitator speed and CO_2 flow rate. Under similar experimental conditions, the extent of Na^+ desorption by CO_2 acidification was found to be slightly lower than that achieved by sulfuric acidification. The equilibrium distribution of Na^+ in the solution and the fibre phase can be estimated using a model based on the Donnan theory.

1. Introduction

The greater demand of environmentally friendly processes in the pulp and paper industry generates a need to replace existing chlorine-based process with oxygen-based processes for bleaching chemical pulps. Unfortunately the selectivity of oxygen-based bleaching processes depends on the deactivation or removal of metal ions in the pulp fibres. Acidification, which provides the source of proton for the replacement of metal ions sorbed on fibres, is one of the most effective methods to remove metal ions from the fibres. The use of mineral acids has disadvantages due to corrosion problem and the increasingly stringent environmental regulations on mill effluents and discharges [1]. Dissolved CO_2 in water forms a weak acid named carbonic acid. The carbonic acid provides an alternative proton source for acidification with less corrosion risk. CO_2 acidification method has been used in some commercial applications [2] and the addition of CO_2 in pulp washing to lower the pH become a common practice in North European and North American Kraft mill [3]. However, details of the kinetics and thermodynamics of the process, particularly the application in the pulp and paper industry, have not been reported. The CO_2 to be dissolved can be obtained from the mill effluent itself. Therefore, using CO_2 for pulp acidification is not only eliminate the cost of chemical, but also solve the problems regarding CO_2 disposal.

Wood fibres carry a negative charge when suspended in water due to the presence of ionisable acidic groups in the hemicelluloses, lignin, and cellulose [4,5]. The main ionisable groups of fibres are carboxyl groups, sulphonic acid groups, catecholic groups, phenolic groups, and hydroxylic groups [6]. Typically, the negative charge sites attract cations and ion exchange could happen [7].

$$\text{Fibre}^-\text{X}^+ + \text{Y}^+ \leftrightarrow \text{Fibre}^-\text{Y}^+ + \text{X}^+ \quad (1)$$

Under an acidic condition proton plays an important role in the displacement of cations from the fibres. Among the ionisable groups the carboxylic group ionises in neutral or weakly acidic conditions, while the phenolic group ionises in alkaline condition. The alcoholic hydroxyl groups are weak acids; therefore they are only ionised in a presence of a strong alkali [7].

The aim of this paper is to develop a method based on thermodynamic and mass transfer principles for studying the kinetics and equilibrium of Na^+ exchange in pulp fibres using CO_2 acidification.

2. Model development for CO_2 acidification

There are three mechanistic steps involved in CO_2 acidification. The first step is the transfer of CO_2 from the gas phase into the liquid phase. The second step is the formation of carbonic acid from the hydrolysis of the CO_2 in the liquid phase. The last step is the exchange of proton with the metal ions sorbed in the fibres.

* Corresponding author. Tel.: +62 271 3060648.
E-mail addresses: denny_vitasari@ums.ac.id, denny.vitasari@gmail.com (D. Vitasari).

1385-8947/$ – see front matter © 2009 Elsevier B.V. All rights reserved.
doi:10.1016/j.cej.2009.03.008

2.1. Mass transfer aspects of CO_2 acidification

The mass transfer in gas–liquid systems are normally characterised by the volumetric mass transfer coefficient [8]. In sparged agitated vessels, at high stirring speeds, it was claimed that k_La was dependent on stirring speed but not the gas flow rate [9]. The use of theoretical equations for determining the volumetric mass transfer coefficient in stirred tank is very limited because of the complexity of the fluid dynamics involved [8]. Most of the models in the literature for predicting this coefficient are empirical correlations based on experimental data.

The volumetric mass transfer coefficient depends on the dimensions of the reactor, physical properties of the liquid and gaseous components in the reactor, degree of mixing and the superficial gas flow rate to the reactor. A list of these correlations was published by Lemoine and Morsi [10]. Some of these correlations were applicable to the prediction of k_La for mass transfer of CO_2 into water in gas sparging reactors.

Perez and Sandall [11] developed the correlation applied to CO_2 dispersion in water and carbopol solution. The experiments were conducted at atmospheric pressure, 297–308 K, superficial gas velocity of 0.162–0.466 ms^{-1}, and reactor diameter of 0.15 m.

$$\frac{d_{imp}^2 k_L a}{D_{AB}} = 21.2\left[\frac{\mu_{eff}}{\rho_L D_{AB}}\right]^{0.5}\left[\frac{\mu_G}{\mu_{eff}}\right]^{0.694}\left[\frac{d_{imp}^2 N\rho_L}{\mu_{eff}}\right]^{1.11} \times \left[\frac{U_G d_{imp}}{\sigma}\right]^{0.447} \quad (2)$$

where k_La is the volumetric mass transfer coefficient (s^{-1}); D_{AB} is the molecular diffusivity of gas in the solvent ($m^2\,s^{-1}$); μ_{eff} is the effective viscosity (Pa s); ρ_L is the density of liquid ($kg\,m^{-3}$); μ_G is the viscosity of gas (Pa s); d_{imp} is the impeller diameter (m); N is the agitation speed (Hz); U_G is the superficial CO_2 velocity (ms^{-1}); and σ is surface tension of the liquid ($N\,m^{-1}$).

Another empirical model for predicting k_La of CO_2 in water was developed by Robinson and Wilke [12]. The experiments were conducted at atmospheric pressure, agitation speeds of 6.7–36.7 Hz and superficial gas velocity of 1–4.6 × 10^{-3} ms^{-1}. In this model k_La was correlated to the specific agitation power and gas superficial velocity:

$$k_La = 3.89\times10^{-3}\times\left(\frac{P_G{}^*}{V_L}\right)^{0.74}U_G^{0.36} \quad (3)$$

where $(P_G{}^*/V_L)$ is the total power input per unit volume of the system (or specific power) ($W\,m^{-3}$).

Matsumura et al. [13] developed a model which took into account the gas hold up factor and the specific agitation power. This correlation was established using data obtained at atmospheric pressure, agitation speed of 7–16.5 Hz, gas superficial velocity of 0.5–10 × 10^{-3} ms^{-1}, and reactor diameter of 0.218 m.

$$\frac{k_La}{\sqrt{D_{AB}}} = 3.09\times10^2\times\left(\frac{P_G{}^*}{V_L}\right)^{0.6}\varepsilon_G^{0.6} \quad (4)$$

where ε_G is the gas hold up.

2.2. Thermodynamic aspects of CO_2 dissociation

As CO_2 dissolves into water it forms carbonic acid, which dissociates to form hydrogen ion and the bicarbonate ion:

$$CO_{2(aq)} + H_2O_{(l)} \leftrightarrow H_2CO_{3(aq)} \leftrightarrow H^+{}_{(aq)} + HCO_3{}^-{}_{(aq)} \quad (5)$$

The equilibrium constant of the reaction is:

$$K_1 = \frac{[H^+][HCO_3{}^-]}{[CO_2]} \quad (6)$$

This equation implies that the availability of proton for the ion exchange depends on the solubility and the transfer rate of CO_2 into the liquid phase.

2.3. Desorption of Na^+ due to acidification

The Donnan theory [14], which was developed based on thermodynamic principles, is commonly used to determine the cation distribution in fibre slurry. Thermodynamically, the distribution of ions in two contacting phases reaches equilibrium when the total free energy is equal to zero. Previously the Donnan theory was used to explain the distribution of ions over an impermeable membrane. It has been later shown that the same principle of distribution can also be applied to systems where the confinement of some ionic species is caused, not by a membrane, but by a macromolecular structure, such as wood fibre wall [4].

The outcome of Donnan theory applied to a slurry of wood fibres could be represented by Eq. (7) below:

$$\lambda = \frac{[H^+]_f}{[H^+]_s} = \sqrt[z]{\frac{[M^{z+}]_f}{[M^{z+}]_s}} = \sqrt[z]{\frac{[I^{z-}]_s}{[I^{z-}]_f}} \quad (7)$$

where λ is distribution coefficient, H^+ represents the hydrogen ion and variables M and I represent different species of cations and anions, respectively. The subscripts f and s denote the concentrations of the species in the fibres and in the solution phases, respectively [15].

Duong et al. [4] developed a model for prediction of the ion exchange capacity of wood fibres based on the Donnan theory and the following assumptions:

(i) Charges inside and outside of fibre wall are neutral.
(ii) Only monovalent anionic species existed in the slurry.
(iii) Both carboxylic and phenolic groups are present in the fibre wall.

Assumptions (i) and (ii) are similar to those of Towers and Scallan's [15] and can be expressed by Eqs. (8) and (9):

$$\sum[A^-]_f + \sum[I^-]_f = [H^+]_f + \sum z_k \sum[M^{z_i+}]_f \quad (8)$$

$$\sum[I^-]_s = [H^+]_s + \sum z_k \sum[M^{z_i+}]_s \quad (9)$$

where $[A^-]_f$ is the effective concentration of the ionised group bound within the fibre wall; z_k is the valence of cation k other than hydrogen present.

Combining Eqs. (7)–(9) gives

$$\lambda = \frac{[I^-]_s}{[I^-]_f} = \frac{[H^+]_s + \sum[M^+]_s + 2\sum[M^{2+}]_s}{[H^+]_f + \sum[M^+]_f + 2\sum[M^{2+}]_f - \sum[A^-]_f} \quad (10)$$

The value of $[A^-]_f$, amount of the ionised group in the fibres, in Eq. (10) could be calculated using the dissociation constant of the ionised groups in the fibres as presented in Eq. (11):

$$K = \frac{[A^-]_f[H^+]_f}{[AH]_f} = \frac{[A^-]_f[H^+]_f}{C/F - [A^-]_f} \quad (11)$$

where C is the acid group content (mol/kg pulp) and F is the water content (L/kg pulp) of the fibre wall. The total amount of the ionised groups in the fibres can be calculated using Eq. (12) below:

$$\sum_{i=1}^{2}[A^-]_f = \sum_{i=1}^{2}\frac{K_i(C_i/F)}{K_i[H^+]_f} \quad (12)$$

The value of $[M^{z+}]_s$ in Eq. (10) can be calculated from the total balance of the cations in the system using Eq. (13):

$$[M^{z+}]_s = \frac{[M^{z+}]_t}{V + F(\lambda^z - 1)} \quad (13)$$

A spreadsheet model was developed to determine the distribution coefficient, λ, by solving Eqs. (10), (12), and (13) simultaneously.

The Donnan equilibrium model requires the intrinsic dissociation constant of the ionisable groups of the pulp fibres. These constants can be calculated using the model developed by Herrington and Petzold [16]:

$$pK_{app} = m\,\text{anti-log}(\alpha) + (pK_a - m) \quad (14)$$

where

$$pK_{app} = pH - \log(\alpha) \quad (15)$$

$$\alpha = \frac{[A^-]}{[HA]} \quad (16)$$

α can be obtained from the potentiometric titration curve, and m is the slope of pK_{app} vs. anti-log (α). pK_a can be calculated using Eq. (14) when α, m, and pK_{app} are known.

3. Experimental procedures

3.1. Pulp preparation

The pulp used in this study was an unbleached eucalyptus kraft pulp of Kappa 19. Initially, the pulp was protonised at pH 2 using 0.01 M HCl. The protonisation required at least 16 h. The protonised pulp was then washed with deionised water until the pH of filtrate reached ~6. The washed pulp was then impregnated with 1 g/L NaCl solution at 1% consistency for 16 h. The pH of the slurry was adjusted to 12 by adding 1 M NaOH solution to transform the pulp to Na form. After 16 h of impregnation, the Na-form pulp was then washed with deionised water until the pH of the filtrate dropped to ~6. The pulp was then dewatered to 25 ± 2% consistency before being stored in the refrigerator at ~4 °C.

3.2. Determination of fibre charge

Approximately 0.5 g of the washed protonised pulp was dispersed in 100 mL of 0.005 M HCl in 1 mM NaCl. The charge of the pulp was then determined by potentiometric titration with 0.05 M NaOH in 1 mM NaCl, using a 718 STAT Titrino titrator at room temperature. During the titration, nitrogen gas was used as a blanket to avoid the dissolution of air into the sample. The titration was performed by a high-precision, microprocessor-controlled autotitrator at temperature of 25 °C. The pH of the slurry was recorded every 30 s. The slurry was homogenized using a magnetic stirrer with a Teflon rod. The rate of the titrant addition was 0.2 mL/min. The blank titration curve was also determined using a 100 mL blank solution consisting of 0.005 M HCl in 1 mM NaCl and a titrant of 0.05 M NaOH in 1 mM NaCl. The fibre charge was calculated using Eq. (17):

$$q = 1000V\frac{c}{w} \quad (17)$$

where q is the fibre charge (mmol/kg), V is the volume difference of titrant used for the sample and for the blank solution (mL), c is the titrant concentration (mol/L) and w is the weight of dry pulp (g).

3.3. Acidification of Na-form pulp with CO_2

The CO_2 acidification experiments were conducted in a bubble reactor. The reactor is a column of 19 cm diameter. The reactor had four baffles of 3 cm wide and was equipped with a turbine agitator for gas dispersion. The diameter of the impeller was 8 cm and there were three impellers. The CO_2 was introduced through a gas diffuser at 5 cm above the bottom of the reactor.

Initially, the CO_2 was delivered to the reactor containing 15 L of deionised water at a predetermined flow rate to reduce the pH of the water to ~4. When the pH reached equilibrium, the pulp was added to form a fibre slurry of 0.15% consistency. The acidification tests were performed at room temperature with an agitator speed set within 300–1200 rpm and CO_2 flow rate within 1–8 L/min. The pH of the slurry was measured every 15 min. Samples of the slurry were taken at 1 and 40 min of the acidification. The acidified fibres were separated from the slurry by filtration using a Büchner funnel. Both fibres and filtrate were then tested for sodium content using Atomic Absorption Spectroscopy (AAS).

3.4. Acidification of Na-form pulp with H_2SO_4

Additional acidification with H_2SO_4 was also carried out for comparison purpose. The experiment was carried out in a stirred tank reactor of 12 cm diameter having four baffles each with 1.2 cm width. Agitation was provided using a stirrer with a single flat-blade turbine impeller of 4 cm diameter. The vessel was submerged in a constant temperature bath during the experiments. The experimental conditions were within the following ranges: pH 2–7, temperature 298–308 K and agitator speed 600–1200 rpm. The pulp was acidified at 0.15% stock consistency. After 40 min of acidification the acidified fibres were filtered from the slurry. Both the fibres and filtrate were subsequently tested for sodium content using AAS.

3.5. Determination of sodium content

The ash of fibres (subjected to 575 ± 25 °C for at least 9 h) was dissolved to form a solution for the Na^+ tests using an Atomic Absorption Spectrophotometer (Model Varian SpectrAA400) following TAPPI standard method T266 om-94. The tests were carried out with air–acetylene fuel and the lamp current set at 5 mA. For tests on the fibres and filtrate, the wavelengths were set at 330.3 and 589.0 nm; and the standard solution matrix was 0–40 and 0–2 ppm, respectively.

The concentration of Na^+ in the fibres was calculated using Eq. (18):

$$M_f = \frac{A_{Mf} - ((W_{pw} - W_{pod})C_{Ms} \times 10^{-3})}{W_{fod}} \times 10^3 \quad (18)$$

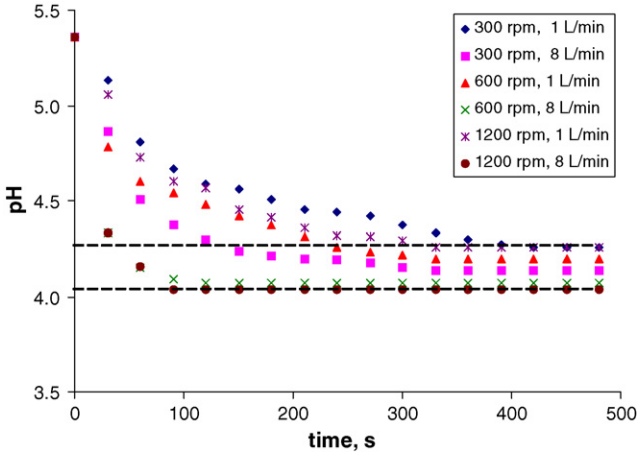

Fig. 1. Effect of CO_2 flow rate and agitation speed on the equilibrium pH.

Table 1
Experimental conditions of CO_2 dissociation used in different studies.

	Perez–Sandall	Robinson–Wilke	Matsumura	This study
Pressure (atm)	1	1	1	1
Agitation speed (Hz)	3.0–8.0	6.7–36.7	7.0–16.0	5.0–20.0
Gas flow rate (ms^{-1})	0.162–0.466	$1–4.6 \times 10^{-3}$	N/A	$5.9–47 \times 10^{-4}$
Tank diameter (m)	0.150	0.150	0.218	0.190

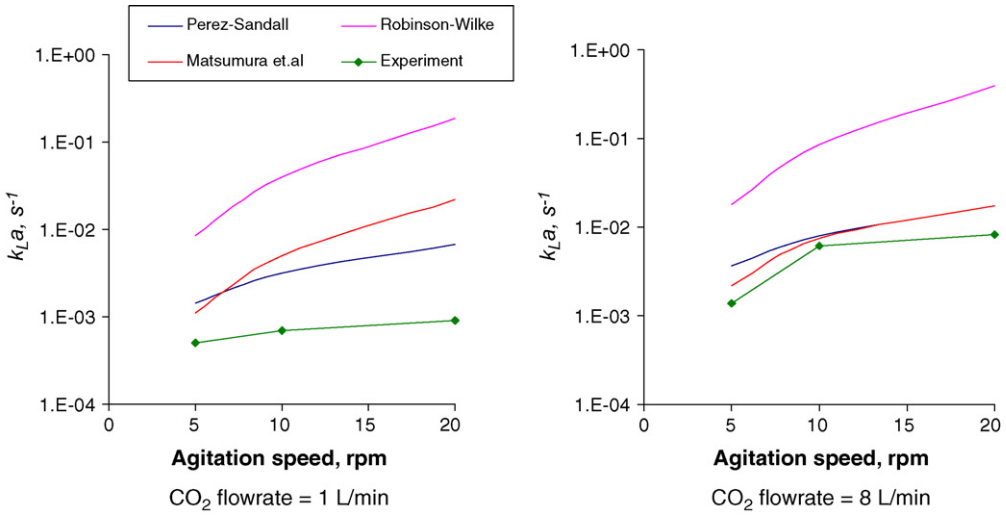

Fig. 2. Comparison of experimental and empirical k_La values at CO_2 flow rates of 1 and 8 L/min.

where M_f is concentration of Na^+ in the fibres (mg/o.d. kg); A_{Mf} is amount of Na^+ in the fibres after the filtration (mg); W_{pw} is total weight of pulp and filter paper after the filtration (g); W_{pod} is the oven-dried weight of fibres and filter paper (g); C_{Ms} is the concentration of Na^+ in the solution (mg/l); and W_{fod} is the oven-dried weight of fibres (g).

3.6. *Yates' algorithm for analysis of factors influencing the extent of Na^+ desorption by CO_2 and H_2SO_4 acidification*

The Yates' algorithm, which is a method to determine effects and interactions of variables observed in factorial experiments [17], was used to determine the factors affecting the kinetics and equilibrium of CO_2 acidification.

4. Results and discussion

4.1. *Effect of CO_2 flow rate on the k_La value*

Fig. 1 shows the equilibrium pH under different CO_2 flow rates and agitator speeds without the presence of fibres. The results indicated that the pH reached equilibrium within the range of 4.0–4.3. The literature value of pK_1 for the dissociation reaction, according to Eq. (5), is 6.37 at 298 K [18]. Using this pK_1 value and a CO_2 solubility value of 0.0324 mol/L at atmospheric pressure and 298 K, one could arrive at a theoretical equilibrium pH of 3.93.

Experimental volumetric mass transfer coefficient, k_La, was calculated based on the mass balance of CO_2 in the gas and liquid phases. The experimental k_La value was then compared with those calculated using empirical correlations established by Perez and Sandall [11], Robinson and Wilke [12], and Matsumura et al. [13]. A summary of the experimental conditions of these studies is provided in Table 1.

Fig. 2 presents k_La values for the CO_2 flow rates of 1 and 8 L/min. It is apparent that the k_La value was higher at 8 L/min, indicating the better transfer of CO_2 from the gas to the liquid phase subjected to higher mass transfer driving force. The difference between the experimental and calculated values of k_La was most likely due to the dissimilarity of the experimental conditions. In this study, the Reynolds number was estimated at $\sim 10^6$ and the Power number at 4, corresponding to a high degree of turbulence in the reactor [19].

4.2. *Mass transfer aspects of Na^+ exchange during CO_2 acidification of pulp fibres*

Once the equilibrium pH of water was achieved, the Na-form pulp was introduced into the reactor for the acidification. The pH during the acidification was monitored and shown in Fig. 3. The results showed that the CO_2 acidification was extremely fast and it was difficult to collect the representative samples. It was apparent that the acidification reached the equilibrium pH within 10 min. The results showed that at higher CO_2 flow rate, the equilibrium

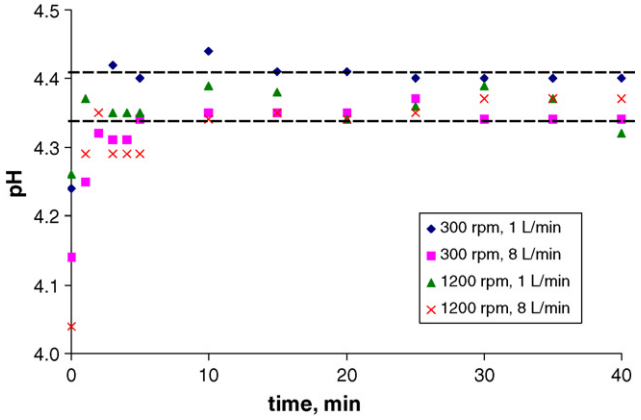

Fig. 3. Changes in pH during CO_2 acidification of pulp fibres under different process conditions.

Table 2
Yates' algorithm analysis of metal removal in CO_2 pulp acidification (t is acidification time, min; Q is CO_2 flow rate, L/min; N is agitation speed, rpm).

Exp	Variables			% Na removed	Cycle 1	Cycle 2	Cycle 3	Divisor	Effect	Estimated effects
	t	N	Q							
y1	1	300	1	90.73	187.53	374.54	755.59	8	94.4	Average
y2	40	300	1	96.80	187.01	381.06	14.19	4	3.5	t
y3	1	1200	1	92.16	188.74	8.76	3.07	4	0.8	N
y4	40	1200	1	94.85	192.32	5.44	−4.86	4	−1.2	tN
y5	1	300	8	92.64	6.07	−0.52	6.52	4	1.6	Q
y6	40	300	8	96.10	2.69	3.58	−3.32	4	−0.8	tQ
y7	1	1200	8	95.17	3.46	−3.38	4.10	4	1.0	NQ
y8	40	1200	8	97.15	1.98	−1.48	1.91	4	0.5	tNQ

pH is lower, indicating the higher level of proton available for the acidification.

4.3. Yates' algorithm analysis of desorption of Na^+ by CO_2 acidification

The Yates' algorithm was used to evaluate the effect of acidification conditions on the desorption of Na^+ from the fibres. The conditions, the responses and final effects of each combinations of the acidification are listed in Table 2. The values of the effect indicated that the extent of the desorption increased with the acidification time, CO_2 flow rate and agitation speed. It was evident that the Na^+ removal was extremely fast and effective (>90.73%), therefore this method of analysis may not be appropriate to distinguish clearly the effect of each process conditions on the extent of the ion exchange during the acidification.

4.4. Comparison of the extent of Na^+ desorption by CO_2 and H_2SO_4 acidification

The extents of the Na^+–H^+ exchange by CO_2 and H_2SO_4 acidification (at 298 K and an agitation speed of 1200 rpm) are shown in Fig. 4. The results show that ~99% of Na^+ could be desorbed by the H_2SO_4 acidification. With CO_2, the degree of desorption was slightly less at ~97%. It should be noted that about 40% of Na^+ was desorbed when the pulp was washed with deionised water at pH ~7.

4.5. Application of Donnan theory to predict the Na^+ distribution in fibres and solution

The distribution coefficient for Na^+ in the fibre slurry was predicted using Eq. (10). The content and the dissociation constant of the carboxylic groups were determined using the data obtained from the potentiometric titrations. It was assumed here that the content of the phenolic groups in the pulp fibres was similar to those found previously by the researchers of our group [1]. The successive steps of the determination of λ are as follows.

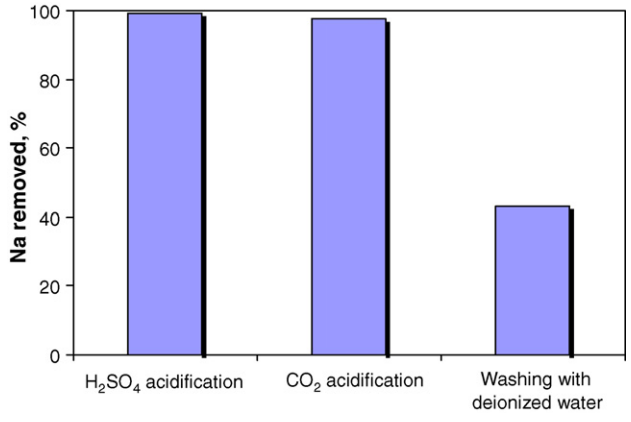

Fig. 4. Amount of Na^+ removed from fibres by treatment with H_2SO_4, CO_2, and deionised water.

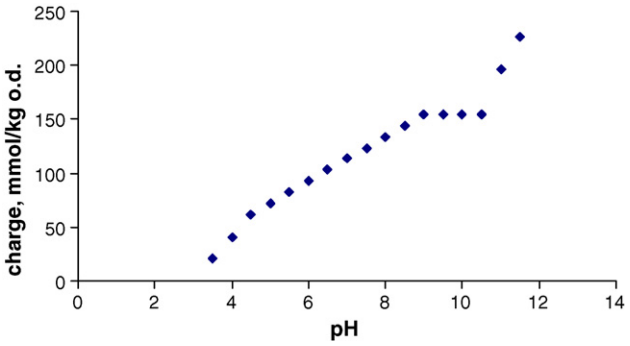

Fig. 5. The charge determined from the potentiometric titration data.

The charge of the fibres at a particular pH was determined using the potentiometric titration curve and Eq. (17). The result of the determination is presented in Fig. 5.

The dissociation constant at pH below 7 was determined from the plot of anti-log α vs. pK_{app} using data from Fig. 5. The values of pK_{app} and α were calculated using Eqs. (15) and (16), respectively. pK_a was determined using Eq. (14) from the intercept of the trendline equation in Fig. 6. This value of pK_a was found to be 3.96.

A spreadsheet model was established to predict the equilibrium distribution coefficient, λ, for Na^+ by solving Eqs. (10), (12), and (13) simultaneously. The equilibrium distribution prediction was compared with the experimental distribution results and shown in Fig. 7. The difference between the experimental and the predicted equilibrium distribution values at pH < 4 appears to be large. This suggests that either the experimental conditions for Na^+ exchange were not ideally at equilibrium or there were errors associated with the sampling and analysis due to the instantaneous nature

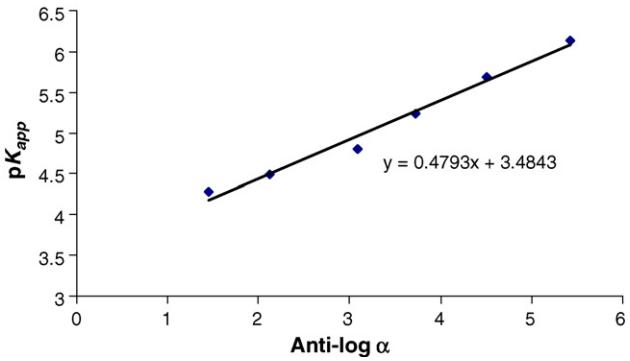

Fig. 6. Relationship between pK_{app} and anti-log α.

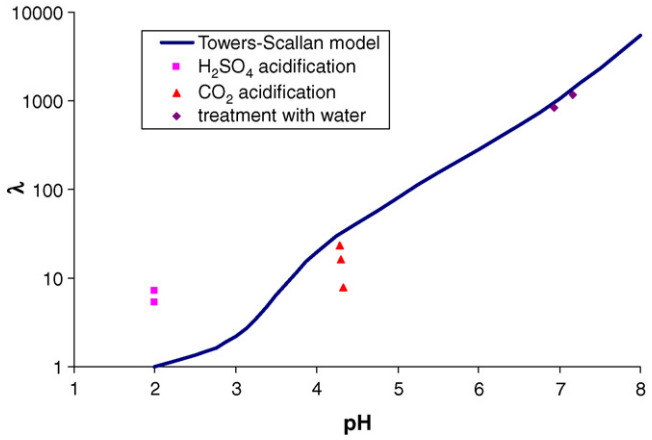

Fig. 7. Comparison of the experimental and calculated distribution coefficient.

of the acidification. In general, the Towers–Scallan model was able to approximate the Na^+ distribution in the fibre and in the adjacent solution at equilibrium.

5. Conclusions

Kinetically, at $Re > 10^4$ and N_p of 4 the dissociation of CO_2 in the aqueous phase was very fast and equilibrium was achieved within 300 s. The volumetric mass transfer coefficient, k_La, of CO_2 from the gas to the liquid phase was in the range of 0.0025–0.0132 s^{-1}.

Thermodynamically, the CO_2 acidification was achievable only at pH > 4.

The extent of Na^+ desorption increased with the agitator speed and CO_2 flow rate. ~97% of Na^+ could be desorbed by CO_2 compared with ~99% Na^+ desorbed by H_2SO_4 acidification under similar experimental conditions.

Due to the instantaneous nature of the desorption of Na^+ during the acidification, the Yates algorithm, which was used to quantify the effects of acidification conditions on the Na^+ desorption, could not discriminate the effects of each factor clearly.

The equilibrium distribution coefficient for Na^+ could be approximated using a model derived from the Donnan theory.

References

[1] Z. Xiong, X. Zhang, H. Wang, F. Ma, L. Li, W. Li, Application of brown-rot basidiomycete *Fomitopsis* sp. IMER2 for biological treatment of black liquor, Journal of Bioscience and Bioengineering 104 (2007) 446–450.
[2] H. Pakarinen, H. Leino, Benefits of using carbon dioxide in the production of DIP containing newsprint, in: 9th PTS-CTP Deinking Symposium, Munich, Germany, May 9–12, 2000.
[3] M. Bannett, M. Ogston, K. Steel, Experiences in Fibreline pH Control Using Carbon Dioxide at the Visy Tumut VPP9 Mill 61st Appita Annual Conference and Exhibition, Appita Inc., Gold Coast, 2007, pp. 63–67.
[4] T.D. Duong, M. Hoang, K.L. Nguyen, Extension of Donnan theory to predict calcium ion exchange on phenolic hydroxyl sites of unbleached kraft fibres, Journal of Colloid and Interface Science 276 (2004) 6–12.
[5] T.D. Duong, M. Hoang, K.L. Nguyen, Sorption of Na+, Ca2+ ions from aqueous solution onto unbleached kraft fibers—kinetics and equilibrium studies, Journal of Colloid and Interface Science 287 (2005) 438–443.
[6] T. Lindstrom, Electrokinetics of the papermaking chemistry, in: J.C. Roberts (Ed.), Paper Chemistry, Blackie Academic & Professional, Glasgow, 1996.
[7] E. Sjostrom, The origin of charge on cellulosic fibers, Nordic Pulp & Paper Research Journal 2 (1989) 90–93.
[8] F.F. Garcia-Ochoa, E. Gomez, Theoretical prediction of gas–liquid mass transfer coefficient, specific area and hold-up in sparged stirred tanks, Chemical Engineering Science 59 (2004) 2489–2501.
[9] J.H. Lee, N.R. Foster, Measurement of gas–liquid mass transfer in multi-phase reactors, Applied Catalysis 63 (1990) 1–36.
[10] R. Lemoine, B.I. Morsi, An algorithm for predicting the hydrodynamic and mass transfer parameters in agetated reactors, Chemical Engineering Journal 114 (2005) 9–31.
[11] J.F. Perez, O.C. Sandall, Gas absorption by non-Newtonian fluids in agitated vessels, American Institute Chemical Engineering Journal 20 (1974) 770–775.
[12] C.W. Robinson, C.R. Wilke, Simultaneous measurement of interfacial area and mass transfer coefficients for a well-mixed gas dispersion in aqueous electrolyte solutions, AIChE Journal 20 (1974) 285.
[13] M. Matsumura, H. Masunaga, J. Kobayashi, Gas absorption in an aerated stirred tank at high power input, Journal of Fermentation Technology 57 (1979) 107–116.
[14] F.G. Donnan, A.B. Harris, The osmotic pressure and conductivity of aqueous solutions of congo-red and reversible membrane equilibria, Journal of Chemical Society 99 (1911) 1554.
[15] M. Towers, A.M. Scallan, Predicting the ion-exchange of kraft pulps using Donnan theory, Journal of Pulp and Paper Science 22 (1996) J332–J337.
[16] T.M. Herrington, J.C. Petzold, An investigation into the nature of charge on the surface of papermaking woodpulps. 1. Charge/pH isotherms, Colloids and Surfaces A: Physicochemical and Engineering Aspects 64 (1991) 97–108.
[17] C.R. Hicks, J. Kenneth, V. Turner, Fundamental Concepts in The Design of Experiments, 5th ed., Oxford University Press, Inc., New York, 1999.
[18] R.L. Jungas, Best literature values for the pK of carbonic and phosphoric acid under physiological conditions, Analytical Biochemistry 349 (2006) 1–15.
[19] E.L. Paul, V.A. Atiemo-Obeng, S.M. Kresta, Handbook of Industrial Mixing, John Wiley & Sons, Inc., New Jersey, 2004.